

## Epigenetic programming at the *Mogat1* locus may link neonatal overnutrition with long-term hepatic steatosis and insulin resistance

Marta Ramon-Krauel,<sup>\*,1</sup> Thais Pentinat,<sup>\*,1</sup> Vincent W. Bloks,<sup>†</sup> Judith Cebrià,<sup>\*</sup> Silvia Ribo,<sup>\*</sup> Ricky Pérez-Wienese,<sup>\*</sup> Maria Vilà,<sup>\*</sup> Ivonne Palacios-Marin,<sup>\*</sup> Antonio Fernández-Pérez,<sup>‡,§,2</sup> Mario Vallejo,<sup>‡,§</sup> Noèlia Téllez,<sup>‡,¶</sup> Miguel Àngel Rodríguez,<sup>‡,||</sup> Oscar Yanes,<sup>‡,||</sup> Carles Lerin,<sup>\*</sup> Rubén Díaz,<sup>\*</sup> Torsten Plosch,<sup>#,3</sup> Uwe J. F. Tietge,<sup>†,3</sup> and Josep C. Jimenez-Chillaron<sup>\*,4</sup>

<sup>\*</sup>Endocrinology Department, Institut de Recerca Sant Joan de Déu, Esplugues, Barcelona, Spain; <sup>†</sup>Department of Pediatrics, Section of Molecular Metabolism and Nutrition, and <sup>‡</sup>Department of Obstetrics and Gynaecology, University Medical Center Groningen, University of Groningen, Groningen, The Netherlands; <sup>§</sup>Ciber de Diabetes y Enfermedades Metabólicas Asociadas (CIBERDEM), Instituto de Salud Carlos III, Madrid, Spain; <sup>¶</sup>Instituto de Investigaciones Biomédicas Alberto Sols, Consejo Superior de Investigaciones Científicas y Universidad Autónoma de Madrid (CSIC/UAM), Madrid, Spain; <sup>||</sup>Bellvitge Biomedical Research Institute (IDIBELL) L'Hospitalet, Barcelona, Spain; and <sup>||</sup>Department of Electronic Engineering, Universitat Rovira i Virgili, Tarragona, Spain

**ABSTRACT:** Postnatal overfeeding increases the risk of chronic diseases later in life, including obesity, insulin resistance, hepatic steatosis, and type 2 diabetes. Epigenetic mechanisms might underlie the long-lasting effects associated with early nutrition. Here we aimed to explore the molecular pathways involved in early development of insulin resistance and hepatic steatosis, and we examined the potential contribution of DNA methylation and histone modifications to long-term programming of metabolic disease. We used a well-characterized mouse model of neonatal overfeeding and early adiposity by litter size reduction. Neonatal overfeeding led to hepatic insulin resistance very early in life that persisted throughout adulthood despite normalizing food intake. Up-regulation of monoacylglycerol *O*-acyltransferase (*Mogat1*) conceivably mediates hepatic steatosis and insulin resistance through increasing intracellular diacylglycerol content. Early and sustained deregulation of *Mogat1* was associated with a combination of histone modifications that might favor *Mogat1* expression. In sum, postnatal overfeeding causes extremely rapid derangements of hepatic insulin sensitivity that remain relatively stable until adulthood. Epigenetic mechanisms, particularly histone modifications, could contribute to such long-lasting effects. Our data suggest that targeting hepatic monoacylglycerol acyltransferase activity during early life might provide a novel strategy to improve hepatic insulin sensitivity and prevent late-onset insulin resistance and fatty liver disease.—Ramon-Krauel, M., Pentinat, T., Bloks, V. W., Cebrià, J., Ribo, S., Pérez-Wienese, R., Vilà, M., Palacios-Marin, I., Fernández-Pérez, A., Vallejo, M., Téllez, N., Rodríguez, M. À., Yanes, O., Lerin, C., Díaz, R., Plosch, T., Tietge, U. J. F., Jimenez-Chillaron, J. C. Epigenetic programming at the *Mogat1* locus may link neonatal overnutrition with long-term hepatic steatosis and insulin resistance. *FASEB J.* 32, 6025–6037 (2018). www.fasebj.org

**KEY WORDS:** neonatal overfeeding · nutritional epigenetics · childhood obesity

**ABBREVIATIONS:** ChIP, chromatin immunoprecipitation; DAG, diacylglycerol; FFA, free fatty acid; H3K27me3, histone 3 lysine-27 trimethylated; H3K4me3, histone 3 lysine-4 trimethylated; H3K9Ac, histone 3 lysine-9 acetylated; LL, large litter; MOGAT, monoacylglycerol acyltransferase; NAFLD, nonalcoholic fatty liver disease; NEFA, nonesterified fatty acid; PPAR $\alpha$ , peroxisome proliferator-activated receptor  $\alpha$ ; PPAR $\gamma$ , peroxisome proliferator-activated receptor  $\gamma$ ; qPCR, quantitative PCR; SL, small litter; TAG, triacylglycerol; VLDL, very low-density lipoprotein

<sup>1</sup> These authors contributed equally to this work.

<sup>2</sup> Current affiliation: Centro para el Desarrollo Tecnológico e Industrial (CDTI), Madrid, Spain.

<sup>3</sup> These authors contributed equally to this work.

<sup>4</sup> Correspondence: Institut de Recerca Sant Joan de Déu, c/Santa Rosa 39-57, 3a Planta, Esplugues, 08950 Barcelona, Spain. E-mail: jjimenezc@isjd.org

doi: 10.1096/fj.201700717RR

This article includes supplemental data. Please visit <http://www.fasebj.org> to obtain this information.

The rising prevalence of obesity is a worldwide health concern because it contributes to the incidence of a wide array of chronic diseases, including cardiovascular disease, type 2 diabetes, and several types of cancer (1, 2). The developmental origins of health and disease hypothesis proposes that critical periods of early development, including the prenatal period and early neonatal life, strongly influence health outcomes throughout life (3, 4). Under this paradigm, rapid weight gain during infancy is associated with childhood obesity and is a major risk factor for cardiovascular disease, nonalcoholic fatty liver disease (NAFLD), or type 2 diabetes during adulthood (5, 6). In humans, the main drivers of rapid neonatal weight gain are overfeeding and/or high calorie intake, which are exemplified by infant formula *vs.* breastfeeding, or high-protein formula *vs.* low-protein formula (7).

While the association between infant nutrition and growth with late-onset hepatic steatosis and insulin resistance is well documented, the causal molecular mechanisms are not fully understood. It has been proposed that epigenetic mechanisms, including DNA methylation and/or histone modifications, might underlie the long-lasting effects associated with early nutritional cues (8, 9).

Litter size reduction during the suckling period is a useful model to study the long-term effects of early overnutrition and rapid neonatal growth. Rodents raised in small litters (SLs) are consistently overfed during lactation and develop late-onset obesity, hepatic steatosis, insulin resistance, impaired glucose tolerance, and renal and cardiac metabolic alterations (10). The long-term metabolic derangements caused by neonatal overfeeding are likely due to a combination of disturbances in the CNS, which may alter food intake (11–13), and the peripheral tissues (14–17).

Hepatic steatosis is characterized by the accumulation of lipid droplets in the cytoplasm of hepatocytes. Two major pathways are involved in hepatic lipid synthesis: the glycerol-3-phosphate pathway (*i.e.*, *de novo* lipogenesis) and the monoacylglycerol acyltransferase (MOGAT) pathway (18). The MOGAT enzymes catalyze the conversion of monoacylglycerol to diacylglycerol (DAG), which is sequentially converted into triacylglycerol (TAG) (19). Under normal physiologic conditions, the MOGAT pathway is marginally active in the liver, and the expression of the 2 key genes of the pathway, *Mogat1* and *Mogat2*, are almost absent. In contrast, the MOGAT pathway is strikingly up-regulated under pathologic conditions, including obesity and NAFLD (19, 20). In these 2 pathologies, *Mogat1* shows strong up-regulation in humans and animal models, suggesting a potential involvement in the accumulation of intrahepatic TAG (21, 22).

We have previously developed a mouse model of neonatal overfeeding and accelerated growth during lactation by litter size reduction (23). Offspring of SLs developed obesity, had impaired glucose tolerance, and experienced insulin resistance with aging. In the present study, we aimed to gain further insight about the tissue or tissues contributing to peripheral insulin resistance, the pathways involved, and the mechanisms that mediate long-term effects. We show that in our SL model the liver strongly contributed to overall insulin resistance. Indeed, hepatic insulin sensitivity deteriorated as early as during the lactation period and persisted until adulthood. Furthermore, hepatic *Mogat1* expression was strikingly up-regulated in 15-d-old SL mice, and this elevation persisted until age 6 mo. *Mogat1* might contribute, at least partially, to the development of both NAFLD and insulin resistance in SL mice. Finally, we found that dynamic specific histone modifications seem to contribute to long-lasting alterations in *Mogat1*.

## MATERIALS AND METHODS

### Animal care and experimental design

The protocols were approved by the Universitat de Barcelona Animal Care and Use Committee. The ICR mouse strain (ICR-CD1; Envigo, Huntingdon, United Kingdom) was chosen for this

study because of its fast somatic growth during the neonatal period. After delivery, litter size was adjusted to 8 pups in the control group, 4 pups in the SL group, or 12 pups per female in the large litter group (LL). Offspring was nursed freely and weaned at 3 wk to standard chow, which was provided *ad libitum* (2014 Teklad Global; Envigo). At weaning, control, SL, and LL mice were housed in groups of 6 mice per cage. SL males and females developed similar pathophysiologic characteristics: accelerated postnatal growth, late-onset obesity, glucose intolerance, and hyperinsulinemia. However, the females did not develop NAFLD with aging (data not shown). Therefore, here we have only included males because the main objective of this work was to understand the mechanisms underlying hepatic NAFLD and hepatic insulin resistance.

### Food intake

Neonatal food intake was determined in 7-d-old neonates as previously described (23). Briefly, at 9:00 AM, the whole litter was removed from the mother and denied access to food for 2 h. Next, the pups were accurately weighed and reintroduced to the mother for 1 h. After the 1 h refeeding period, the cohorts were weighed again. Differences in body weight are a good estimate of food intake.

Adult food intake was determined in 1- and 4-mo-old individual mice. Food was weighed every 24 h for 5 consecutive days. The data were averaged and corrected for body weight to determine daily food intake. Furthermore, an independent group of mice was placed individually in closed cages connected to a Phenomaster Labmaster System (TSE Systems, Hamburg, Germany). Food and water were available *ad libitum*, and measurements represent the mean intake over 1 wk.

### Biochemical analyses

Serum insulin was determined by ELISA (MilliporeSigma, Burlington, MA, USA). Serum triglycerides and free fatty acids (FFAs) were measured using the Triglyceride Assay Kit (MilliporeSigma) and the Nonesterified Fatty Acid (NEFA) Kit (Roche, Basel, Switzerland), respectively. Whole blood glucose was measured with a Glucose Meter Elite (Menarini, Barcelona, Spain).

### Milk composition

Milk was obtained at d 15.5 of lactation from an independent set of dams (control,  $n = 4$ ; SL,  $n = 4$ ). Milk was collected under anesthesia (pentobarbital, 40 mg/kg) by massage. Triglycerides, glycerol, and FFAs were determined by colorimetric methods. Total protein concentration was determined in diluted samples with the Pierce BCA Protein Assay Kit (Pierce; Thermo Fisher Scientific, Waltham, MA, USA). Relative lactose concentration was determined by liquid chromatography [(Acquity Ultra-Performance Liquid Chromatography Ethylene Bridged Hybrid Hydrophilic Interaction Chromatography (UPLC BEH HILIC) column; Waters, Milford, MA, USA)] coupled to mass spectrometry (QqQ/MS 6490; Agilent Technologies, Santa Clara, CA, USA).

### Epididymal fat mass assessment

Epididymal fat depots were dissected and fat mass calculated as a percentage of wet tissue per whole body weight.

### In vivo metabolic testing

Intraperitoneal glucose (2 g/kg weight) tolerance tests were performed in unrestrained conscious mice after a 12-h food

deprivation. Glucose was monitored at 0, 15, 30, 60, and 120 min after glucose administration. Glucose tolerance was calculated as the area under the glucose curve.

### Insulin action

*In vivo* tissue-specific insulin sensitivity was assessed in 15-d-old, 1-mo-old, and 4-mo-old mice as follows. Fifteen-day-old mice were separated from the dam for 4 h before the test. Insulin (1 U) was administered as an intraperitoneal bolus into anesthetized mice (pentobarbital, 40 mg/kg). Tissue extraction was conducted 15 min after insulin injections. Adult mice were denied access to food overnight (12 h). One unit of insulin was administered *via* the vena cava into anesthetized mice. Tissues were collected 2 min after the infusion and snap frozen in liquid nitrogen. Tissues were stored at  $-80^{\circ}\text{C}$  until Western blot analyses were performed.

### Liver TAG and DAG content

Liver TAG content was determined as previously described (24). Briefly, livers (50 mg) were homogenized in ice-cold PBS. Hepatic lipids were extracted according to Bligh and Dyer (25). Hepatic triglycerides were quantified using a Triglyceride Assay Kit (Roche Diagnostics, Indianapolis, IN, USA).

Liver DAG content was measured by NMR analysis. Briefly, the chloroform phase was isolated, dried, and reconstituted in 700  $\mu\text{l}$  of 2:1  $\text{CD}_3\text{Cl}:\text{CD}_3\text{OD}$  with 4%  $\text{D}_2\text{O}$  and 0.01% tetramethylsilane (TMS) solution (0.067 mM).  $^1\text{H}$  NMR spectra were recorded at 300K on an Advance III 600 spectrometer (Bruker, Bremen, Germany). After preprocessing and visual checking of the NMR data set, specific  $^1\text{H}$  regions of DAGs were identified and quantified in the spectra using the AMIX 3.9 software package (Bruker).

### *In vivo* lipogenesis

*In vivo* lipogenesis was determined following a previously published general protocol (26). Briefly, 2% w/w sodium ( $1\text{-}^{13}\text{C}$ )-acetate solution (99 atom %, Isotec; MilliporeSigma) was added to the drinking water of mice for 5 consecutive days. At the end of this period, animals were humanely killed. Livers were quickly removed, freeze clamped, and stored at  $-80^{\circ}\text{C}$ . Liver homogenates were prepared in PBS, and C17:0 was added as internal standard. Lipids were hydrolyzed in HCl/acetonitrile (1:22 v/v), and fatty acids were extracted in hexane and derivatized using Br-2,3,4,5,6-pentafluorobenzyl/acetonitrile/triethanolamine (1:6:2 v/v). Incorporation of the [ $^{13}\text{C}$ ] label into newly synthesized fatty acids was determined using an Agilent 5975 series GC-MS spectrometer (Agilent Technologies). The normalized mass isotopomer distributions measured by GC-MS (m0–mx) were corrected for natural abundance of [ $^{13}\text{C}$ ]. Using mass isotopomer distribution analysis, algorithms for isotope incorporation into the shown fatty acids either by synthesis or chain elongation were calculated.

### Hepatocyte isolation and culture

Hepatocytes were isolated from 12-h unfed mice. Briefly, the mice were anesthetized with ketamine and xylazine. The liver was perfused through the cava vein with 10 ml of HBSS (MilliporeSigma) during 4 min. Next, the collagenase solution [0.04% (w/v), 5 ml; MilliporeSigma] was perfused during 2 more minutes. At the end of the digestion, the liver was carefully removed and cells were filtered through 100- $\mu\text{m}$

nylon filters for 50 ml conical tubes (Sardstedt, Nümbrecht, Germany) and washed 2 times with cold HBSS (600  $\mu\text{g}$ , 10 min,  $4^{\circ}\text{C}$ ; 70  $\mu\text{g}$ , 2 min,  $4^{\circ}\text{C}$ ). Hepatocytes were suspended in DMEM, supplemented with 10% (v/v) fetal bovine serum, 100 nM insulin (MilliporeSigma), and then seeded onto 6 multiwell plates treated with 0.1% collagen solution (MilliporeSigma) at a final density of  $1 \times 10^6$  cells per well. After 4 h, the media were replaced with fresh DMEM containing 25 mM glucose, 1% fetal bovine serum, and 100 nM insulin for 24 h until the experiments were performed.

### FFA incorporation into TAG

Hepatocytes were washed with HBSS and incubated in DMEM without fetal bovine serum and insulin but containing FFAs (0.4 mM palmitate and 0.4 mM oleate; MilliporeSigma) conjugated with a solution containing 3% bovine serum albumin. Cells were incubated for 24 h in this medium. At the end of each manipulation, cell monolayers were suspended in 500  $\mu\text{l}$  of SDS 0.1%, and TAG was extracted and analyzed as previously described.

### *In vivo* very low-density lipoprotein secretion

Secretion of very low-density lipoproteins (VLDLs) *in vivo* was assessed by measuring the progressive accumulation of TAG in serum of mice treated with tyloxapol (MilliporeSigma). Intraperitoneal injection of tyloxapol (500 mg/kg body weight) was performed on conscious mice after food was withheld for 4 h. Blood samples were obtained from the tail vein at 0, 90, and 180 min after tyloxapol administration.

### Real-time quantitative PCR analysis

cDNA was synthesized from 1  $\mu\text{g}$  of total RNA using Random Primers (Promega Biotech Ibérica, Madrid, Spain). The amplification of the genes of interest was performed using real-time quantitative PCR (qPCR) on a 7500 Real Time PCR System and 7500 v.2.0.4 software (Thermo Fisher Scientific) using SYBR (Promega Biotech Ibérica) Master Mix. Data were normalized with cyclophilin. The primers are listed in Supplemental Table 1.

### Assessment of DNA methylation by mass spectrometry

Genomic DNA was isolated using DNAzol (Promega Biotech Ibérica). The quantitative analysis of 5-meC levels of the 5' regions of *Mogat1* was determined after bisulfite treatment (EZ DNA Methylation Kit; Zymo Research, Orange, CA, USA) by using the Sequenom EpiTyper (Sequenom, San Diego, CA, USA). Bisulfite-treated genomic DNA was amplified using 2 pairs of primers (Supplemental Table 2). The methylation level at each CpG site for each sample was calculated as the percentage of the methylated alleles over the sum of methylated and unmethylated alleles.

### Western blot analyses and chromatin immunoprecipitation

Western blot analyses were performed using 50  $\mu\text{g}$  of protein extract as previously described (27). Likewise, chromatin immunoprecipitation (ChIP)-qPCR analyses were performed as previously described (28). Briefly, histone binding was

determined as the immunoprecipitation/input ratio and further corrected by the IgG to establish the background. Finally, the data were presented as fold change over control in order to compare the environmental impact of early nutrition and growth on the 3 histones that we wished to analyze. The list of antibodies is provided in Supplemental Table 3.

### Statistical analysis

Results are expressed as means  $\pm$  SEM. When samples showed normal distribution and similar standard variations, statistical analysis was performed by 2-tailed Student's *t* test or 1-way ANOVA as indicated (RStudio v.0.98.1102). Normal distribution was assessed by the Shapiro-Wilk test and confirmed visually through Q-Q graphs. The Mann-Whitney-Wilcoxon test was applied to nonnormally distributed data. A value of  $P < 0.05$  was considered significant.

## RESULTS

### SL mice develop metabolic syndrome features very early in life

Mice from SLs (Fig. 1A) developed many features of the metabolic syndrome as adults, including obesity, dyslipidemia, and glucose intolerance (23). We aimed to identify early pathophysiologic and molecular events to explain long-term programming of hepatic steatosis and insulin resistance. We began by confirming that by 2 wk of age, SL mice were heavier (Fig. 1B) and displayed greater adiposity than controls (Fig. 1C). Rapid neonatal growth might be explained by increased food intake (Fig. 1D) and

differences in macronutrient milk content (Fig. 1E). Specifically, by lactation d 15, total TAG content was 2-fold higher in milk from SL females as compared to controls (Fig. 1E). In contrast, the concentration of lactose, protein, NEFAs, and glycerol remained similar between groups (Fig. 1E). Following this early dietary pattern, serum glucose and NEFAs were also significantly elevated in 2-wk-old SL mice (Table 1). In contrast, the concentration of insulin and TAG were similar among groups (Table 1).

Strikingly, food and water intake normalized in SL mice after weaning, as determined at 1 and 4 mo of life (Supplemental Fig. 1A, B). Despite normalizing feeding behavior, SL mice remained heavier than controls (23). Likewise, SL mice developed dyslipidemia and hepatic TAG accumulation by age 1 mo (Fig. 1F and Table 1), before the onset of hyperinsulinemia and impaired glucose tolerance (Table 1).

### Hepatic MOGAT pathway is significantly increased in SL mice

Next, we aimed to study the pathway or pathways that might contribute to increase liver TAG content in SL mice (Fig. 2A). Expression of key lipogenic genes remained largely unaltered in livers of young and adult SL mice, and *Fasn* expression even decreased in adult SL mice (Fig. 2B). Instead, we found significant differences in expression of genes involved in the MOGAT pathway (Fig. 2C). Remarkably, *Mogat1* was already 3-fold higher in lactating SL mice compared to control mice and was further increased (up to 20-fold) with aging. Other genes in this pathway

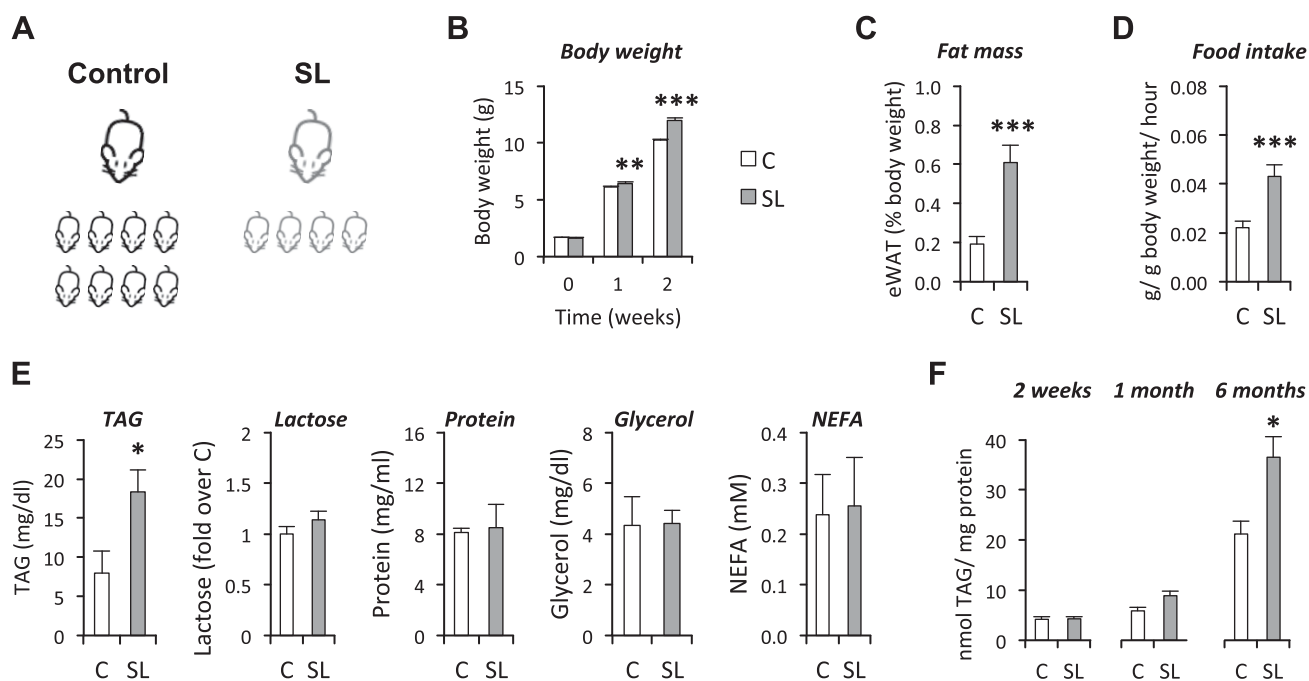


**Figure 1.** Early physiologic adaptations in SL mice. *A*) Protocol of litter size adjustments during lactation period. *B*) Body weight of control (C) and SL mice from birth to second week of life ( $n \geq 28$ ; 3 control litters; 8 SL litters). *C*) Epididymal fat mass of C ( $n = 26$ ; 3 litters) and SL ( $n = 19$ ; 5 litters) mice at age 2 wk. *D*) Food intake in 1-wk-old mice (C,  $n = 16$ , 2 litters; SL,  $n = 11$ , 3 litters). *E*) Total TAG, lactose, protein, glycerol, and FFAs were determined in whole milk samples at lactation d 14.5. C,  $n = 4$ , 1 litter; SL,  $n = 5$ , 1 litter. *F*) Intrahepatic triglyceride content was determined in lactating 2-wk-old mice ( $n = 10$ ; 2 litters), 1-mo-old mice ( $n = 20$ ; 5 litters), and 6-mo-old mice ( $n \geq 6$ ; at least 2 litters). All values are means  $\pm$  SEM. \* $P < 0.05$ , \*\* $P < 0.01$ , \*\*\* $P < 0.001$  (Student's *t* test).

TABLE 1. Serum metabolites determined in C and SL mice

Metabolite	2 wk			1 mo			4 mo		
	C	SL	P	C	SL	P	C	SL	P
Glucose (mg/dl)	67 ± 5.3	102 ± 16.7	0.051	50.27 ± 3.41	40.53 ± 2.13	0.015	54.62 ± 2.45	51.88 ± 3.11	0.49
Insulin (ng/ml)	0.133 ± 0.033	0.11 ± 0.023	0.70	0.093 ± 0.017	0.098 ± 0.013	0.82	0.15 ± 0.02	0.25 ± 0.03	0.013
TAG (mg/dl)	6.08 ± 0.73	5.81 ± 0.43	0.75	32.69 ± 2.59	43.37 ± 3.30	0.012	88.15 ± 7.99	130.4 ± 22.07	0.03
NEFAs (mM)	0.37 ± 0.017	0.60 ± 0.074	<0.001	ND	ND		0.37 ± 0.036	0.44 ± 0.009	0.08
Area under curve (a.u.)	ND	ND		1.00 ± 0.08	0.91 ± 0.08	0.39	1.00 ± 0.16	1.60 ± 0.17	0.01
Liver (g)	0.39 ± 0.025	0.45 ± 0.015	0.04	1.24 ± 0.031	1.32 ± 0.030	0.05	2.46 ± 0.058	2.75 ± 0.097	0.01
Liver (% body weight)	3.68 ± 0.118	3.91 ± 0.080	0.15	3.90 ± 0.077	3.95 ± 0.131	0.76	5.18 ± 0.067	5.03 ± 0.167	0.33

Two-week-old mice were denied access to food for 4 h, whereas 1- and 4-mo-old mice were denied access to food overnight (16 h). A.u., arbitrary units; C, control; ND, not done. Values are means ± SEM. Values of  $P < 0.05$  are considered statistically significant, by Student's  $t$  test.

(*Acs11*, *Acs15*) were significantly elevated in adult mice only (Fig. 2C). Finally, expression of genes that regulate FFA oxidation (*Ppara*, *Cpt1a*, *Cpt2*) and VLDL production/secretion (*Hnf4*, *Mttp*, *Apob*) were unaltered at either 2 wk or 6 mo of age (Fig. 2D, E).

Together, these data suggest that up-regulation of the MOGAT pathway might mediate TAG accumulation in the liver of SL mice. In agreement, *in vitro* incorporation and esterification of FFAs (palmitate and oleate) into TAG was significantly higher in hepatocytes from SL mice compared to controls (Fig. 2F). In contrast, *in vivo de novo* lipogenesis, as assessed by the incorporation of [<sup>13</sup>C]-acetate into the lipid fraction [*i.e.*, palmitate (16:0), stearate (18:0) and oleate (18:1)], was reduced in the liver of young SL mice (Fig. 2G). Finally, *in vivo* VLDL secretion, determined through the progressive accumulation of serum TAG after treatment with tyloxapol, was similar between groups (Fig. 2H). Taken together, our data strongly suggest that the esterification pathway (*i.e.*, MOGAT pathway) is enhanced in SL mice, likely due to altered expression of the genes that regulate the pathway, with *Mogat1* being the gene that shows the strongest dysregulation.

### Increased *Mogat1* is associated with hepatic steatosis and insulin resistance via Diacylglycerol

The MOGAT enzymes regulate TAG synthesis through modulating the intracellular levels of DAG (Fig. 3A). Paralleling increased *Mogat1* expression and predicting TAG accumulation, total DAG was 1.5-fold higher in livers of 2-wk-old SL mice, which moderately persisted until the age of 6 mo (Fig. 3B). Although differences in intracellular DAG content might seem modest, mice fed a high-fat diet for 3 mo also exhibited a 1.5-fold elevation in DAG, while the concentration of TAG was 10-fold higher (Supplemental Fig. 2A). In mice fed a high-fat diet, DAG and TAG content positively correlated with the up-regulation of genes of the MOGAT pathway (Supplemental Fig. 2B).

DAG mediates insulin resistance by decreasing intracellular insulin signaling (29). Accordingly, *in vivo* hepatic insulin action was impaired in 2-wk-old SL mice (Fig. 3C). As expected, insulin stimulated the phosphorylation of Akt, Gsk3, and p70Sk in control mice. However, this effect was completely lost in SL mice (Fig. 3C). Furthermore, basal nonstimulated p-Akt was much higher in the liver of SL mice, which is a primary indication of insulin resistance. Notably, impaired insulin action in the liver persisted in 1- and 4-mo-old SL mice (Fig. 3D).

These data suggest that up-regulation of *Mogat1* might contribute in part to both hepatic steatosis and hepatic insulin resistance *via* DAG synthesis. Additional indirect proof of concept was provided by including a new experimental group: we generated LLs by maintaining 12 neonates per female during lactation (Fig. 4A). As expected, LL mice exhibited blunted neonatal

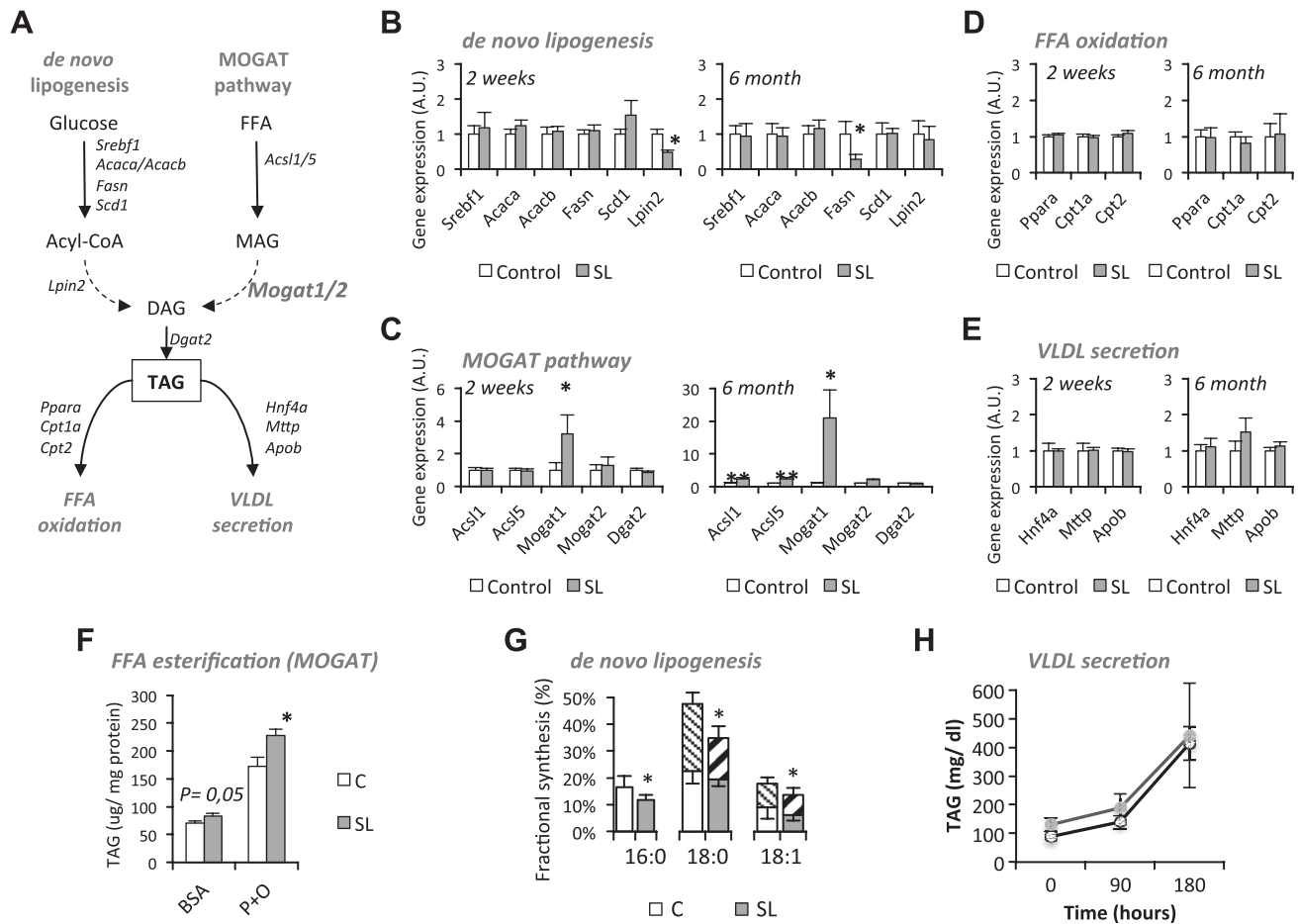


**Figure 2.** Pathways involved in homeostasis of hepatic TAG levels. *A*) Schematic representation detailing pathways involved in TAG synthesis (glycerol 3-P and MOGAT pathway), degradation (FFA oxidation), and export (VLDL secretion). *B*) Expression (mRNA) of key genes of glycerol-3-P pathway (*C*) monoacylglycerol-*O*-acetyl transferase pathway, (*D*) lipid oxidation, and (*E*) VLDL secretion in control (C) and SL mice at 2 wk (C,  $n = 7$ , 3 litters; SL,  $n = 8$ , 3 litters) and 6 mo of life (C,  $n = 5$ , 1 litter; SL,  $n = 6$ , 1 litter). *F*) *In vitro* incorporation of FFAs (palmitate and oleate) into hepatocytes of 6-mo-old C and SL mice (C,  $n = 15$  replicates from 2 independent isolations; SL,  $n = 12$  replicates from 2 isolations). *G*) *In vivo* incorporation of [ $^{13}\text{C}$ ]-acetate into hepatic lipid fraction of C ( $n = 10$ , 3 litters) and SL mice ( $n = 10$ , 3 litters). *H*) *In vivo* VLDL secretion as measured by accumulation of serum TAG after treatment with lipoprotein lipase inhibitor tyloxapol (C,  $n = 12$ , 4 litters; SL,  $n = 9$ , 5 litters). All values are means  $\pm$  SEM. \* $P < 0.05$ , \*\* $P < 0.01$  (Student's *t* test).

growth curves (Fig. 4B) and remained leaner than the controls by age 4 mo (Fig. 4C). Adiposity (epididymal fat) and insulinemia tended to be reduced in LL mice (Supplemental Fig. 3A, B), while glucose tolerance was similar between adult control and LL mice (Supplemental Fig. 3C). Hepatic DAG showed a tendency toward reduced levels ( $P = 0.07$ , Fig. 4D), while TAG content dropped to 30% in LL mice ( $P < 0.05$ , Fig. 4E). Following reduced hepatic lipid content, *Mogat1* mRNA showed modest reductions ( $P = 0.08$ ), while the other genes of the MOGAT pathway remained unaltered (Fig. 4F). Furthermore, markers of lipogenesis (*Srebf1*, *Fasn*, *Acaca*, *Scd1*) and VLDL production (*Apob*) were also similar between groups (Supplemental Fig. 3D). Contrary to observations in SL mice, *Cpt2* was strongly up-regulated in the liver of LL mice, suggesting an additional involvement of FFA oxidation in mediating low TAG content in LL mice (Supplemental Fig. 3D). Finally, *in vivo* insulin signaling was increased in adult LL mice, suggesting improved hepatic insulin sensitivity (Fig. 4G).

### Life-course deregulation of *Mogat1* associates with dynamic histone modifications

Up-regulation of *Mogat1* might be attributed to an increased level of upstream transcription factors, including the peroxisome proliferator-activated receptors  $\alpha$  and  $\gamma$  (PPARA, PPARG) (30, 31). However, protein content and mRNA levels were similar among groups at 2 wk and 6 mo of age (Supplemental Fig. 4A, B). Alternatively, long-term deregulation of gene expression might be attributed to epigenetic modifications (32). We measured the presence of specific histone modifications, through ChIP, that are shown to bind to the proximal regulatory regions of *Mogat1*: histone 3 lysine-4 trimethylated (H3K4me3), histone 3 lysine-9 acetylated (H3K9Ac), and histone 3 lysine-27 trimethylated (H3K27me3) (Fig. 5A). We found that the binding of the 3 histones was relatively poor in the liver of neonates (Supplemental Fig. 5A). After age 2 wk, the signal becomes much stronger for the H3K4me3 and the H3K27me3 marks, which stays at similar levels until age

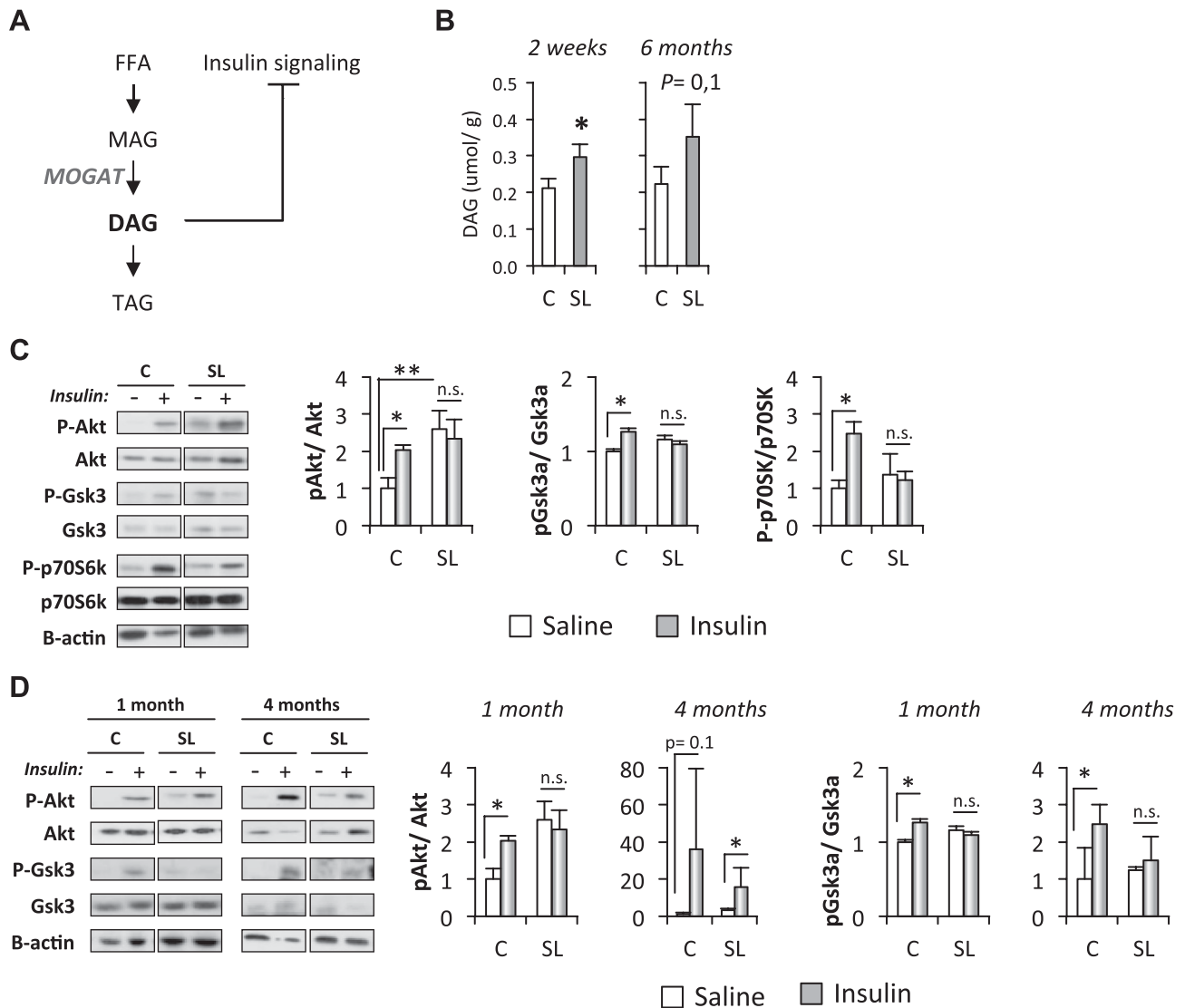


**Figure 3.** MOGAT pathway contributes to impair hepatic insulin signaling *via* DAG accumulation. **A)** MOGAT pathway depicting link between DAG synthesis and insulin signaling. **B)** Hepatic DAG content in young [2 wk; control (C)  $n = 8$ , 6 litters; SL,  $N = 8$ , 7 litters] and adult (6 mo; C,  $n = 5$ , 1 litter; SL,  $N = 6$ , 1 litter) mice. **C)** *In vivo* insulin action in 15 d old C ( $n = 4$ , 3 litters) and SL mice ( $n = 4$ , 3 litters). Images are representative Western blots. Graphs represent quantification of Western blot. White bars represent unstimulated (saline) and gray bars insulin-stimulated samples. **D)** *In vivo* insulin action in 1- (C,  $n = 4$ , 3 litters; SL,  $n = 5$ , 3 litters) and 4-mo-old mice (C,  $n = 4$ , 3 litters; SL,  $n = 4$ , 3 litters). Images are representative blots and graphs are their quantification. All values are means  $\pm$  SEM. N.s., not significant.  $*P < 0.05$ ,  $**P < 0.01$  (Student's *t* test or Mann-Whitney-Wilcoxon test when samples did not follow normal distribution).

6 mo (Supplemental Fig. 5A). The binding of H3K9Ac is stronger by age 6 mo. In the liver of 24 h neonates, the relative abundance of these 3 histone marks was similar among groups (Supplemental Fig. 5B). However, as early as by age 2 wk, the binding of the repressive mark H3K27me3 was 50% reduced in the liver of SL mice (Fig. 5B). The activating marks H3K4me3 and H3K9Ac were unaltered. By the age of 6 mo, H3K4me3 binding was increased 2-fold in SL mice, whereas H3K9Ac and H3K27me3 remained unaltered (Fig. 5B). Together, this combination conceivably favors increased *Mogat1* gene expression in SL mice throughout their life span (Fig. 6). However, in the liver of LL mice, the combination of histones might favor *Mogat1* repression: the activating histone mark H3K9Ac was significantly reduced by age 2

wk, whereas the repressing mark H3K27me3 showed a nonstatistical trend by age 6 mo (Fig. 5C).

Finally, we measured cytosine methylation in the CpG Island located within the region where we have performed the ChIP assays (Fig. 5A). Globally, the methylation profile of this region was relatively low and similar among control, SL, and LL mice at age 15 d (Fig. 5D, E). Likewise, the pattern of methylation remained similar between control and SL mice at 6 mo of age (Fig. 5D).

## DISCUSSION

Immediate postnatal overfeeding increases the risk for chronic diseases later in life, including obesity, insulin

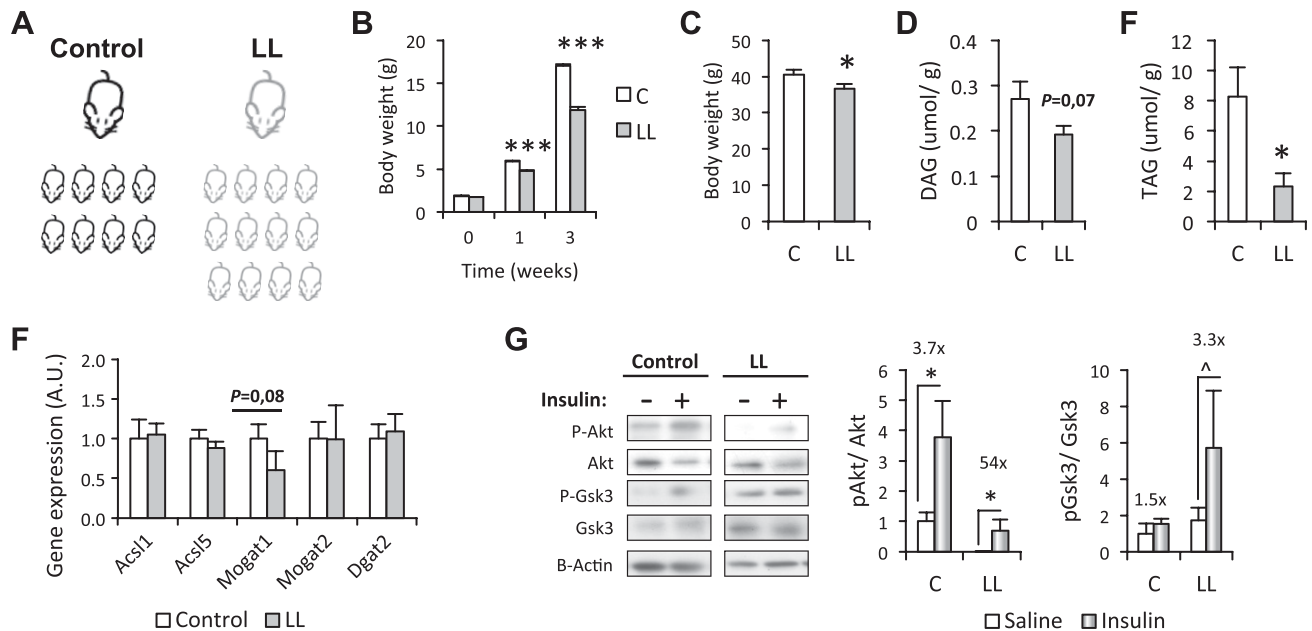


**Figure 4.** Physiologic and metabolic characterization of LL mice. *A*) Scheme representing adjustments in litter size during lactation period: control (C) = 8 pups; LL = 12 pups. *B*) Body weight of C ( $n = 38$ , 8 litters) and LL mice ( $n = 30$ , 5 litters) from birth until weaning. *C*) Body weight of 4-mo-old C ( $n = 6$ , 6 litters) and LL mice ( $n = 6$ , 6 litters). *D*) Hepatic DAG and *E*) TAG content in adult C ( $n = 7$ , 1 litter) and LL mice ( $n = 7$ , 1 litter). *F*) Expression (mRNA) of genes of MOGAT pathway (C,  $n = 8$ , 7 litters; LL,  $n = 7$ , 7 litters). *G*) *In vivo* insulin action in 4-mo-old mice (C,  $n = 5$ , 5 litters; LL,  $n = 5$ , 5 litters). Images are representative blots and graphs are their quantification. All values are means  $\pm$  SEM.  $^{\wedge}P < 0.1$ ,  $*P < 0.05$ ,  $***P < 0.001$  (Student's *t* test or Mann-Whitney-Wilcoxon test when samples did not follow normal distribution).

resistance, hepatic steatosis, and type 2 diabetes (5, 6). We had previously developed a mouse model of neonatal overfeeding and rapid neonatal growth by litter size reduction (23). As adults, mice from SLs developed several components of the metabolic syndrome, including obesity, dyslipidemia, and glucose intolerance. Peripheral insulin resistance was mainly responsible for long-term metabolic dysfunction because  $\beta$ -cell function was preserved in adult SL mice (23). Several studies have pointed to the role of hyperphagia in mediating obesity and obesity-related insulin resistance (11, 12, 14, 33–35). We reported that SL mice exhibited hyperphagia during lactation, which might account for accelerated neonatal growth (Fig. 6A). However, early overfeeding was a transient phenomenon, and calorie intake normalized in SL mice after weaning (11, 15, 36). Therefore, our data strongly suggest that late-onset metabolic dysfunction in SL mice might be largely attributable to deregulation of peripheral functions (*i.e.*, peripheral insulin resistance).

We confirmed that *in vivo* insulin action was already impaired in the liver of 15-d-old SL mice, which persisted until adulthood. Others have also described that litter size reduction increases susceptibility of developing insulin resistance with aging (15, 16, 36, 37). However, we are among the first to show that neonatal overfeeding leads to rapid derangement of insulin sensitivity in a tissue-specific manner (17). Because liver is a key tissue in maintaining whole body homeostasis, impaired hepatic insulin action conceivably contributes to progressive whole body insulin resistance in SL mice. Other tissues, including adipose tissue and skeletal muscle, may additionally contribute to whole body insulin resistance. Clearly it would be useful

to investigate their potential impact to whole body insulin sensitivity in future studies.

We next attempted to understand the molecular mechanisms contributing to hepatic steatosis and insulin resistance in SL mice. We found major alterations in expression of genes of the MOGAT pathway, which might play a key role in mediating both hepatic steatosis and insulin resistance in our mouse model (Fig. 6B) (38). Combined data from SL, control, and LL mice showed that *Mogat1* expression correlated positively with hepatic TAG concentration. Furthermore, functional assays confirmed that hepatic steatosis in SL mice can neither be attributed to enhanced *de novo* lipogenesis nor impaired VLDL secretion. In contrast, hepatocytes of SL mice accumulated more TAG than control hepatocytes on incubation with FFAs (palmitate and oleate). The incorporation of FFAs into the triglyceride fraction occurs primarily through FFA esterification *via* the MOGAT pathway. Therefore, although we cannot completely exclude the notion that part of these FFAs might be oxidized differentially between groups, the overall functional assays and gene expression strongly support that the MOGAT pathway may play a central role in mediating hepatic steatosis in SL mice.

In agreement with this, human observational studies and animal models of obesity confirm that the MOGAT pathway is strikingly up-regulated under pathologic conditions, including obesity and NAFLD (19, 20). Indeed, *Mogat1* is one of the genes of this pathway that shows the strongest up-regulation in both conditions (21, 22).

The MOGAT pathway may be directly involved in the development of hepatic insulin resistance *via* DAG

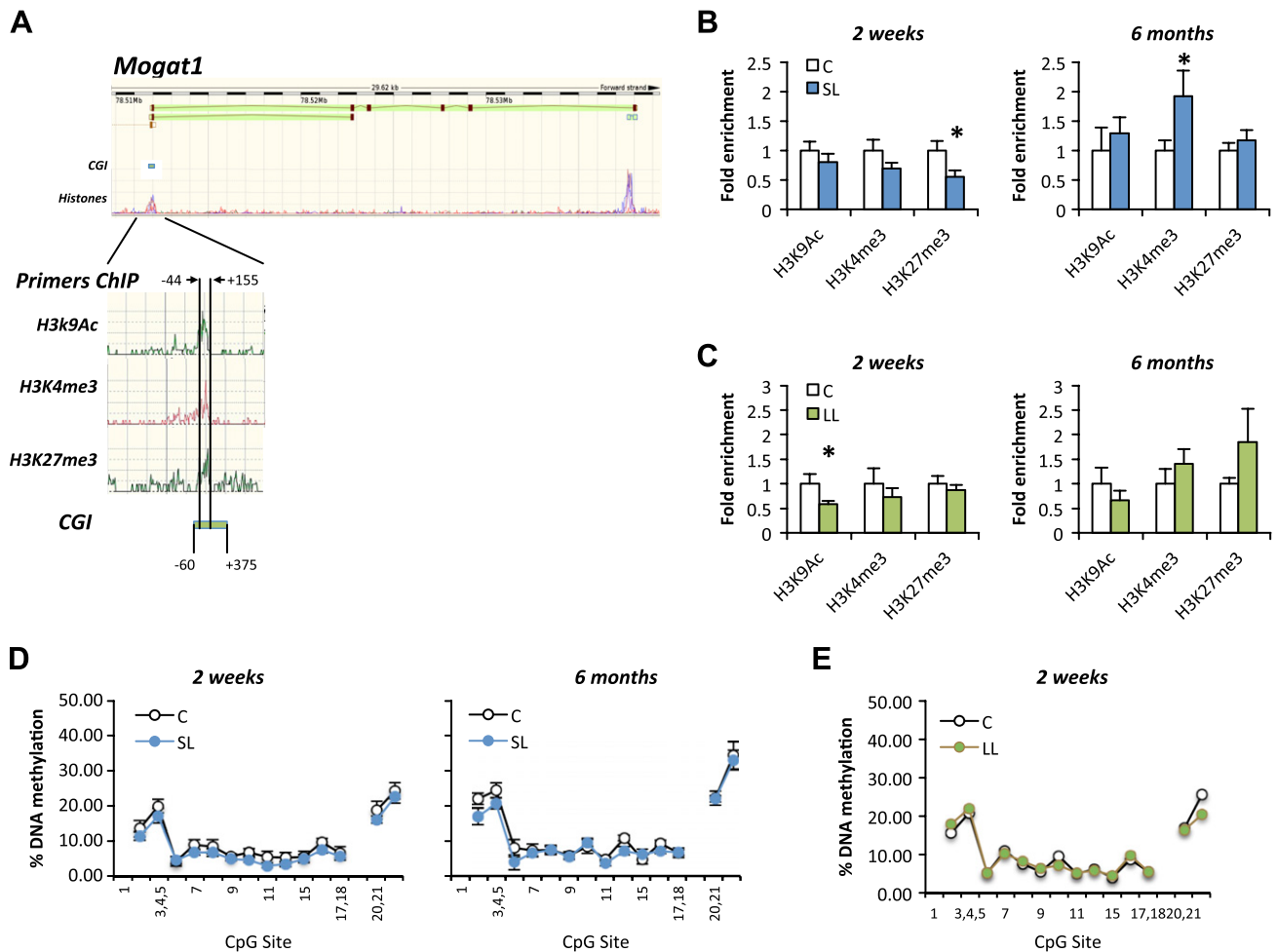


**Figure 5.** Epigenetic regulation of hepatic *Mogat1* expression. **A**) *Mogat1* structure detailing position of CpG island (CGI, green box) and binding sites for 3 histones within 5' regulatory region of gene. Arrows designate position of primers for ChIP-qPCR analysis based on their relative distance to transcription start site. **B**) *In vivo* ChIP-qPCR in liver samples of control (C) and SL mice at 2 wk (C,  $n = 12$ , 6 litters; SL,  $n = 12$ , 6 litters) and 6 mo of age (C,  $n = 9$ , 5 litters; SL,  $n = 9$ , 5 litters). **C**) ChIP-qPCR in liver samples of C and LL mice at 2 wk (C,  $n = 11$ , 3 litters; LL,  $n = 9$ , 3 L) and 6 mo of age (C,  $n = 11$ , 3 litters; LL,  $n = 7$ , 3 litters). **D**) DNA methylation profile of promoter region of *Mogat1*. Cytosine methylation was determined by EpiTyper, and data were represented as percentage methylation across individual CpG sites in proximal region of gene. Two-week-old mice: C,  $n = 6$ , 4 litters; SL,  $n = 6$ , 5 litters; 6-mo-old mice: C,  $n = 5$ , 1 litter; SL,  $n = 6$ , 1 litter. **E**) DNA methylation profile in liver samples of 2-wk-old C ( $n = 5$ , 1 litter) and LL mice ( $n = 5$ , 1 litter). Values are mean  $\pm$  SEM. \* $P < 0.05$ , Wilcoxon test for nonparametric samples.

synthesis (Fig. 6B). DAG may act as a signaling molecule that mediates insulin resistance through impairing Akt phosphorylation (29, 39). Again, combined data from SL and LL mice show a positive correlation between *Mogat1* expression and hepatic DAG concentration. In turn, intrahepatic DAG levels negatively correlated with insulin action. Although these data are associative, they strongly suggest that hepatic insulin resistance is at least partly mediated *via* DAG accumulation. In addition to DAG signaling, other pathways might also mediate insulin resistance, including inflammation. This last one is especially relevant in humans, where it appears closely linked to obesity (40). However, we did not find any evidence involving inflammation in the development of insulin resistance in our model. We speculate that the reasons for lacking inflammation in our obese model include the following. First, the animals were maintained on a standard chow diet, which contains low fat. It is known that high-fat and high-sucrose diets are major inducers of inflammation

in rodents. Indeed, other studies have shown that perinatal overfeeding did not induce inflammation, at least when the animals were maintained on a standard diet (36, 41). Second, and relatedly, we have measured markers of inflammation up to 6 mo of age. It might be possible that inflammation develops later in life. In sum, our model strongly supports a scenario in which obesity and insulin resistance arise in the absence of inflammatory markers. We speculate that inflammation may develop later in life and/or in response to other nutrition factors, such as high-fat feeding.

Overall previous data, including ours, suggests an important role for *Mogat1* in mediating hepatic TAG accumulation and insulin resistance. In agreement, causal functional experiments confirmed that short-term hepatic suppression of *Mogat1* (through RNAi and antisense oligonucleotides) improved hepatic insulin signaling, whole body glucose homeostasis, and moderately reduced TAG content (21, 42). However, in models of obesity, such as

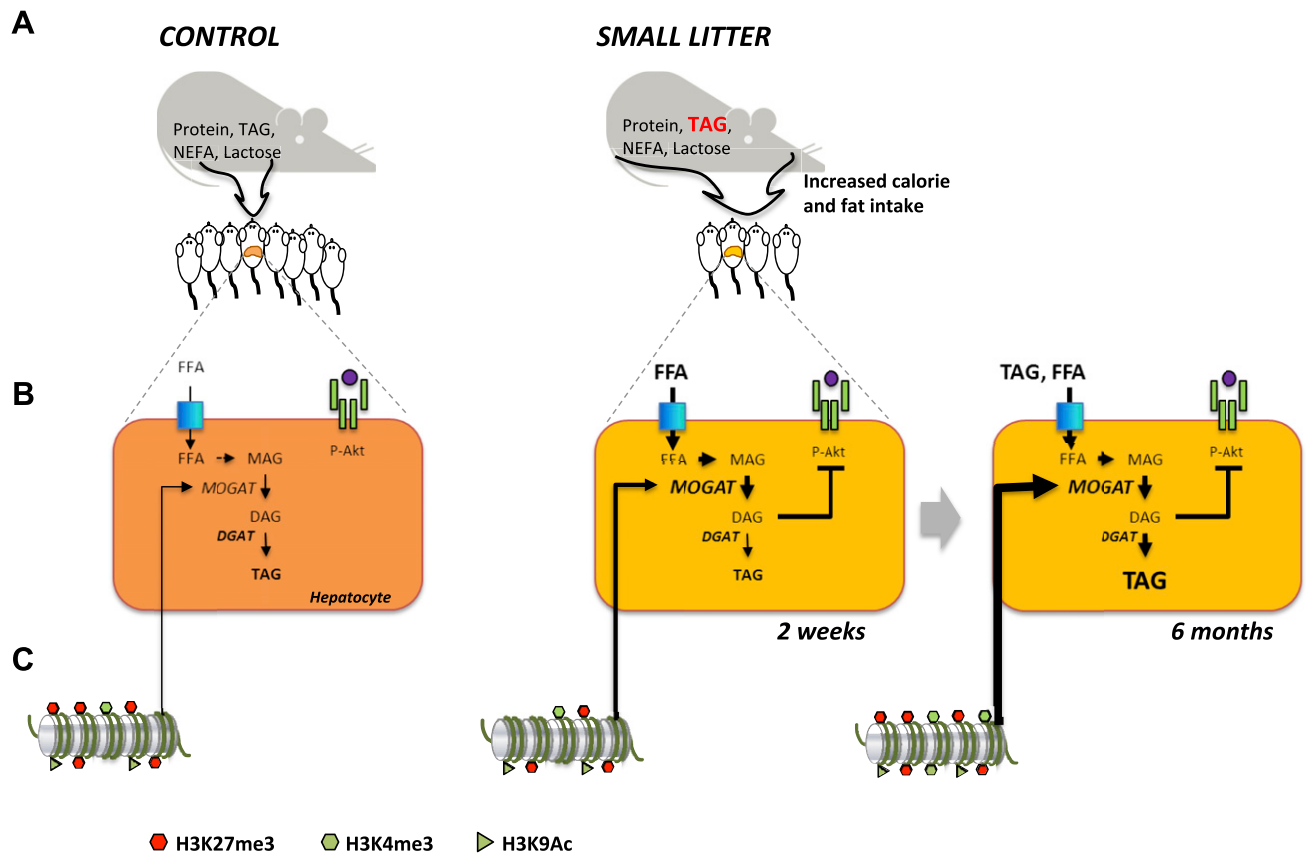


**Figure 6.** A) At 2 wk of life, SL mice are exposed to excess lipid availability as result of combined hyperphagia and increased TAG milk content. B) Increased dietary lipid disposal increased flux of FFAs through MOGAT pathway, which in turn results in augmented levels of intrahepatic DAG and TAG. DAG acts as signaling molecule that impairs insulin signaling at level of Akt. C) Chromatin modifications that lead to early (1) and sustained (2) deregulation of *Mogat1*. In young SL mice, presence of repressing mark H3K27me3 is reduced, which results in less repression of *Mogat1*. In adult mice presence of activating marks H3K4me3 and H3K9Ac is increased, which together might favor chromatin states that allow net expression of gene.

diet-induced obesity and *ob/ob* mice, similar approaches moderately improved glucose tolerance and insulin sensitivity without reducing TAG content (43). This effect could be attributed to the short-term effect of the treatment with the antisense oligonucleotides. Nevertheless, long-term *Mogat1* knockdown did not ameliorate hepatic steatosis and insulin sensitivity in *ob/ob* and lipodystrophic mice (*Agpat2*<sup>-/-</sup>) (44). Together, the previous data suggest that *Mogat1* might be directly involved in liver steatosis and hepatic insulin sensitivity, at least under standard chow feeding conditions. However, in genetic models of obesity (*ob/ob*), lipodystrophy (*Agpat2*<sup>-/-</sup>), or diet-induced obesity, in which the liver accumulates massive amounts of lipids, additional pathways should be involved as well. This explains why strategies aimed to reduce *Mogat1* in adults do not improve hepatic steatosis. Yet our data support a rationale for modulating *Mogat1* early in life before the appearance of fatty liver. This hypothesis deserves future experiments (for example, maintaining LL mice on a high-fat diet), which are, however, beyond the scope of the current work.

We next addressed the potential mechanisms that contribute to sustained deregulation of *Mogat1*. It has been proposed that epigenetic mechanisms might link early environmental cues, including nutrition, with long-lasting

regulation of gene expression (8, 9). Accordingly, neonatal overnutrition (11, 12) or altered milk macronutrient composition (45) is associated with differential DNA methylation patterns in key metabolic organs. However, we did not find differences of cytosine methylation in the transcription start site of *Mogat1*. These data suggest that in our model, DNA methylation does not play a major role in regulating *Mogat1*. Nevertheless, we cannot completely rule out the notion that differences in DNA methylation in other distant regions might influence *Mogat1* expression. Genome-wide cytosine methylation profiling would be a valuable means to explore the potential implication of other regions, which will be further investigated in the future.

The current study found that long-term deregulation of *Mogat1* is attributed in part to the dynamic remodeling of the histones that bind the regulatory region of the gene. Accordingly, histone modifications might favor *Mogat1* expression in SL mice, whereas different combination of histones might repress it in LL mice. In particular, the repressive histone mark H3K27me3 was reduced in liver from 2-wk-old SL mice, suggesting that *Mogat1* is less repressed in young SL mice than in controls. In adult mice, the activating mark H3K4me3 was 2-fold enriched in SL mice (Fig. 6C). However, in young LL mice the

activating mark H3K9Ac was reduced, whereas in old mice the repressive histone H3K27me3 was increased. This combination is associated with permanent reductions of *Mogat1* expression in LL mice. The important findings here are that early patterns of histone modifications were not permanently maintained. Instead, early marks are remodeled throughout the life span in response to environmental factors, including obesity and nutrition.

In agreement with this finding, other models of developmental programming of late-onset diabetes also show striking histone dynamics with aging (46, 47). However, it is relevant to note that SL and LL mice show opposite traits, including whole body physiology, hepatic DAG/TAG levels, and *Mogat1* levels. Yet the histone marks associated with *Mogat1* in each model do not follow the same pattern. For example, in young SL mice *Mogat1* up-regulation associates to reduced H3K27me3, whereas in young LL mice *Mogat1* down-regulation associates to reduced H3K9Ac. Together, these data suggest a complex set of histone interactions in modulating the *Mogat1* expression.

Because we wanted to gain insight into the physiologic signals during early life that contribute to stimulating the MOGAT pathway in the liver of SL mice, we analyzed the macronutrients present in the milk and found that TAG concentration doubled in SL females. Increased milk TAG content correlated with higher concentration of NEFAs in the serum of 15 d old suckling SL mice. Therefore, litter size reduction might lead to increased flux of FFA esterification through the MOGAT pathway (Fig. 6A, B). Strikingly, changes in macronutrient milk composition in response to litter size have been previously reported (17, 35, 36, 48). The signals that lead to changes in macronutrient milk composition are currently unknown. We speculate that reductions in litter size will lead to lower milk production. Furthermore, it is important to note that the milk of rodents is very rich in lipids. Therefore, we propose that lowering milk production as a result of reduced litter size would result in the net accumulation of TAG. Other possibilities include that the cells of the mammary gland may adapt the production and secretion of macronutrients, again in response to offspring demand. This is an area of intense investigation because milk composition in humans, which is exemplified by breast-feeding *vs.* bottle-feeding, influences infant growth and predisposes them to childhood overweight and chronic diseases later in life (49, 50). Still, how may this change in macronutrient content influence *Mogat1* gene expression? There is evidence that, *in vitro*, either FFAs or glucose modify *Mogat1* mRNA. Instead, it has been shown that PPARA and PPARG may regulate hepatic *Mogat1* both in humans and mice (31, 51). However, gene expression and protein content of PPARs were unaltered in SL mice. Therefore, here we propose that up-regulation of *Mogat1* could rely on the transcriptional activity of PPAR proteins, which indeed depends on the chromatin conformations specified by the combination of histones that bind to the promoter region of the gene. Hence, we predict a complex interplay among nutrient availability (FFAs), histone variants (H3K4me3/H3K27me3), and transcription factors (PPARA/G) in

mediating early and long-term expression of *Mogat1*. Finally, in addition to the potential link between TAG/FFAs and the PPARs, it should be noted that SL mice have increased global calorie intake during lactation. Hence, SL mice also have increased carbohydrate and protein intake even though the concentration of these macronutrients is similar in the milk of control and SL dams. Therefore, it could be possible that other signals derived from these macronutrients additionally contribute to regulate *Mogat1* expression in the liver of SL mice. These hypotheses are currently under investigation.

In summary, we show that inappropriate neonatal nutrition may lead to extremely rapid and permanent derangements of insulin action. A conceivable explanation is that developing individuals are exposed to a hyperlipidemic diet due to combined hyperphagia and high milk TAG concentrations (Fig. 6A). Next, increased TAG/FFA intake during lactation would result in enhanced flux of FFAs through the monoacylglycerol pathway, leading to transient DAG levels, which in turn impair insulin signaling (Fig. 6B). Our results indicate that *Mogat1* could be an important player in this process. Long-lasting alterations in *Mogat1* expression are likely attributable to epigenetic reprogramming at the *Mogat1* locus *via* histone modifications (Fig. 6C). Therefore, targeting MOGAT activity in the liver of lactating individuals could be a novel therapeutic strategy to prevent NAFLD and hepatic insulin resistance (31). This opens a rationale for defining a new window of opportunity for potential primary prevention of chronic diseases. Our data are of particular relevance when translated to the arena of human disease because they reinforce the importance of infant nutrition in order to permanently maintain a healthy metabolic balance throughout the life span. FJ

## ACKNOWLEDGMENTS

This work was supported by Instituto de Salud Carlos III (PII4/00035, CP11/00312 to J.J.C.), Ministerio de Economía y Competitividad (BFU2011-29739 to J.J.C.), the Netherlands Organization for Health Research and Development (ZonMW, Grant 91211053 to T.P.), and the Spanish Ministry of Economy and Competitiveness (BFU2014-52149-R to M.V.). I.P.-M. is supported by a National Council for Science and Technology in Mexico (CONACyT) Ph.D. Scholarship. M.R.-K. and T.P. share senior authorship. The authors declare no conflicts of interest.

## AUTHOR CONTRIBUTIONS

M. Ramon-Krauel wrote the report and researched data; T. Pentinat designed the experimental setting and researched data; V. W. Bloks, A. Fernández-Pérez, N. Téllez, and M. À. Rodríguez researched data, and reviewed and edited the report; J. Cebrià, S. Ribo, R. Pérez-Wienese, M. Vilà, and I. Palacios-Marin researched data; M. Vallejo and O. Yanes reviewed and edited the report; C. Lerin, R. Díaz, T. Plosch, and U. J. F. Tietge contributed to discussion, and reviewed and edited the manuscript; and J. C. Jimenez-Chillaron designed the experiments and wrote the manuscript.

## REFERENCES

- Finucane, M. M., Stevens, G. A., Cowan, M. J., Danaei, G., Lin, J. K., Paciorek, C. J., Singh, G. M., Gutierrez, H. R., Lu, Y., Bahalim, A. N., Farzadfar, F., Riley, L. M., and Ezzati, M.; Global Burden of Metabolic Risk Factors of Chronic Diseases Collaborating Group (Body Mass Index). (2011) National, regional, and global trends in body-mass index since 1980: systematic analysis of health examination surveys and epidemiological studies with 960 country-years and 9.1 million participants. *Lancet* **377**, 557–567
- Danaei, G., Finucane, M. M., Lu, Y., Singh, G. M., Cowan, M. J., Paciorek, C. J., Lin, J. K., Farzadfar, F., Khang, Y. H., Stevens, G. A., Rao, M., Ali, M. K., Riley, L. M., Robinson, C. A., and Ezzati, M.; Global Burden of Metabolic Risk Factors of Chronic Diseases Collaborating Group (Blood Glucose). (2011) National, regional, and global trends in fasting plasma glucose and diabetes prevalence since 1980: systematic analysis of health examination surveys and epidemiological studies with 370 country-years and 2.7 million participants. *Lancet* **378**, 31–40
- Gluckman, P. D., Hanson, M. A., and Beedle, A. S. (2007) Early life events and their consequences for later disease: a life history and evolutionary perspective. *Am. J. Hum. Biol.* **19**, 1–19
- Gluckman, P. D., Hanson, M. A., Cooper, C., and Thornburg, K. L. (2008) Effect of *in utero* and early-life conditions on adult health and disease. *N. Engl. J. Med.* **359**, 61–73
- Andersen, L. G., Holst, C., Michaelsen, K. F., Baker, J. L., and Sørensen, T. I. (2012) Weight and weight gain during early infancy predict childhood obesity: a case-cohort study. *Int. J. Obes.* **36**, 1306–1311
- Leunissen, R. W., Kerkhof, G. F., Stijnen, T., and Hokken-Koelega, A. (2009) Timing and tempo of first-year rapid growth in relation to cardiovascular and metabolic risk profile in early adulthood. *JAMA* **301**, 2234–2242
- Oddy, W. H., Mori, T. A., Huang, R. C., Marsh, J. A., Pennell, C. E., Chivers, P. T., Hands, B. P., Jacoby, P., Rzehak, P., Koletzko, B. V., and Beilin, L. J. (2014) Early infant feeding and adiposity risk: from infancy to adulthood. *Ann. Nutr. Metab.* **64**, 262–270
- Jirtle, R. L., and Skinner, M. K. (2007) Environmental epigenomics and disease susceptibility. *Nat. Rev. Genet.* **8**, 253–262
- Jiménez-Chillaron, J. C., Díaz, R., Martínez, D., Pentinat, T., Ramón-Krauel, M., Ribó, S., and Plösch, T. (2012) The role of nutrition on epigenetic modifications and their implications on health. *Biochimie* **94**, 2242–2263
- Habbout, A., Li, N., Rochette, L., and Vergely, C. (2013) Postnatal overfeeding in rodents by litter size reduction induces major short- and long-term pathophysiological consequences. *J. Nutr.* **143**, 553–562
- Li, G., Kohorst, J. J., Zhang, W., Laritsky, E., Kunde-Ramamoorthy, G., Baker, M. S., Fiorotto, M. L., and Waterland, R. A. (2013) Early postnatal nutrition determines adult physical activity and energy expenditure in female mice. *Diabetes* **62**, 2773–2783
- Plagemann, A., Harder, T., Brunn, M., Harder, A., Roepke, K., Wittrock-Staar, M., Ziska, T., Schellong, K., Rodekamp, E., Melchior, K., and Dudenhausen, J. W. (2009) Hypothalamic proopiomelanocortin promoter methylation becomes altered by early overfeeding: an epigenetic model of obesity and the metabolic syndrome. *J. Physiol.* **587**, 4963–4976
- Colliden, G., Bolland, E., Parkash, J., Caron, E., Langlet, F., Prevot, V., and Bouret, S. G. (2014) Neonatal overnutrition causes early alterations in the central response to peripheral ghrelin. *Mol. Metab.* **4**, 15–24
- Glavas, M. M., Kirigiti, M. A., Xiao, X. Q., Enriori, P. J., Fisher, S. K., Evans, A. E., Grayson, B. E., Cowley, M. A., Smith, M. S., and Grove, K. L. (2010) Early overnutrition results in early-onset arcuate leptin resistance and increased sensitivity to high-fat diet. *Endocrinology* **151**, 1598–1610
- Bei, F., Jia, J., Jia, Y. Q., Sun, J. H., Liang, F., Yu, Z. Y., and Cai, W. (2015) Long-term effect of early postnatal overnutrition on insulin resistance and serum fatty acid profiles in male rats. *Lipids Health Dis.* **14**, 96
- Conceição, E. P., Franco, J. G., Oliveira, E., Resende, A. C., Amaral, T. A., Peixoto-Silva, N., Passos, M. C., Moura, E. G., and Lisboa, P. C. (2013) Oxidative stress programming in a rat model of postnatal early overnutrition—role of insulin resistance. *J. Nutr. Biochem.* **24**, 81–87
- Du, Q., Hosoda, H., Umekawa, T., Kinouchi, T., Ito, N., Miyazato, M., Kangawa, K., and Ikeda, T. (2015) Postnatal weight gain induced by overfeeding pups and maternal high-fat diet during the lactation period modulates glucose metabolism and the production of pancreatic and gastrointestinal peptides. *Peptides* **70**, 23–31
- Shi, Y., and Cheng, D. (2009) Beyond triglyceride synthesis: the dynamic functional roles of MGAT and DGAT enzymes in energy metabolism. *Am. J. Physiol. Endocrinol. Metab.* **297**, E10–E18
- Hall, A. M., Kou, K., Chen, Z., Pietka, T. A., Kumar, M., Korenblat, K. M., Lee, K., Ahn, K., Fabbri, E., Klein, S., Goodwin, B., and Finck, B. N. (2012) Evidence for regulated monoacylglycerol acyltransferase expression and activity in human liver. *J. Lipid Res.* **53**, 990–999
- Cortés, V. A., Curtis, D. E., Sukumaran, S., Shao, X., Parameswara, V., Rashid, S., Smith, A. R., Ren, J., Esser, V., Hammer, R. E., Agarwal, A. K., Horton, J. D., and Garg, A. (2009) Molecular mechanisms of hepatic steatosis and insulin resistance in the AGPAT2-deficient mouse model of congenital generalized lipodystrophy. *Cell Metab.* **9**, 165–176
- Hayashi, Y., Suemitsu, E., Kajimoto, K., Sato, Y., Akhter, A., Sakurai, Y., Hatakeyama, H., Hyodo, M., Kaji, N., Baba, Y., and Harashima, H. (2014) Hepatic monoacylglycerol *O*-acyltransferase 1 as a promising therapeutic target for steatosis, obesity, and type 2 diabetes. *Mol. Ther. Nucleic Acids* **3**, e154
- Lee, Y. J., Ko, E. H., Kim, J. E., Kim, E., Lee, H., Choi, H., Yu, J. H., Kim, H. J., Seong, J. K., Kim, K. S., and Kim, J. W. (2012) Nuclear receptor PPAR $\gamma$ -regulated monoacylglycerol *O*-acyltransferase 1 (MGAT1) expression is responsible for the lipid accumulation in diet-induced hepatic steatosis. *Proc. Natl. Acad. Sci. USA* **109**, 13656–13661
- Pentinat, T., Ramon-Krauel, M., Cebria, J., Diaz, R., and Jimenez-Chillaron, J. C. (2010) Transgenerational inheritance of glucose intolerance in a mouse model of neonatal overnutrition. *Endocrinology* **151**, 5617–5623
- Pruis, M. G., Lendvai, A., Bloks, V. W., Zwier, M. V., Baller, J. F., de Bruin, A., Groen, A. K., and Plösch, T. (2014) Maternal western diet primes non-alcoholic fatty liver disease in adult mouse offspring. *Acta Physiol. (Oxf.)* **210**, 215–227
- Bligh, E. G., and Dyer, W. J. (1959) A rapid method of total lipid extraction and purification. *Can. J. Biochem. Physiol.* **37**, 911–917
- Oosterveer, M. H., van Dijk, T. H., Tietge, U. J., Boer, T., Havinga, R., Stellaard, F., Groen, A. K., Kuipers, F., and Reijngoud, D. J. (2009) High fat feeding induces hepatic fatty acid elongation in mice. *PLoS One* **4**, e6066
- Jimenez-Chillaron, J. C., Hernandez-Valencia, M., Reamer, C., Fisher, S., Joszi, A., Hirshman, M., Oge, A., Walrond, S., Przybyla, R., Boozer, C., Goodyear, L. J., and Patti, M. E. (2005) Beta-cell secretory dysfunction in the pathogenesis of low birth weight-associated diabetes: a murine model. *Diabetes* **54**, 702–711
- Martínez, D., Pentinat, T., Ribó, S., Daviaud, C., Bloks, V. W., Cebrià, J., Villalmanzo, N., Kalko, S. G., Ramón-Krauel, M., Díaz, R., Plösch, T., Tost, J., and Jiménez-Chillaron, J. C. (2014) *In utero* undernutrition in male mice programs liver lipid metabolism in the second-generation offspring involving altered Lxra DNA methylation. *Cell Metab.* **19**, 941–951
- Erion, D. M., and Shulman, G. I. (2010) Diacylglycerol-mediated insulin resistance. *Nat. Med.* **16**, 400–402
- Sankella, S., Garg, A., and Agarwal, A. K. (2016) Characterization of the mouse and human monoacylglycerol *O*-acyltransferase 1 (*Mogat1*) promoter in human kidney proximal tubule and rat liver cells. *PLoS One* **11**, e0162504
- Yu, J. H., Song, S. J., Kim, A., Choi, Y., Seok, J. W., Kim, H. J., Lee, Y. J., Lee, K. S., and Kim, J. W. (2016) Suppression of PPAR $\gamma$ -mediated monoacylglycerol *O*-acyltransferase 1 expression ameliorates alcoholic hepatic steatosis. *Sci. Rep.* **6**, 29352
- Gluckman, P. D., Hanson, M. A., Buklijas, T., Low, F. M., and Beedle, A. S. (2009) Epigenetic mechanisms that underpin metabolic and cardiovascular diseases. *Nat. Rev. Endocrinol.* **5**, 401–408
- Habbout, A., Delemasure, S., Goirand, F., Guillard, J. C., Chabod, F., Sediki, M., Rochette, L., and Vergely, C. (2012) Postnatal overfeeding in rats leads to moderate overweight and to cardiometabolic and oxidative alterations in adulthood. *Biochimie* **94**, 117–124
- Kappeler, L., De Magalhães Filho, C., Leneuve, P., Xu, J., Brunel, N., Chatziantoniou, C., Le Bouc, Y., and Holzenberger, M. (2009) Early postnatal nutrition determines somatotrophic function in mice. *Endocrinology* **150**, 314–323
- Fiorotto, M. L., Burrin, D. G., Perez, M., and Reeds, P. J. (1991) Intake and use of milk nutrients by rat pups suckled in small, medium, or large litters. *Am. J. Physiol.* **260**, R1104–R1113
- Liu, Z., Lim, C. Y., Su, M. Y., Soh, S. L., Shui, G., Wenk, M. R., Grove, K. L., Radda, G. K., Han, W., and Xiao, X. (2013) Neonatal

- overnutrition in mice exacerbates high-fat diet-induced metabolic perturbations. *J. Endocrinol.* **219**, 131–143
37. Rodrigues, A. L., De Souza, E. P., Da Silva, S. V., Rodrigues, D. S., Nascimento, A. B., Barja-Fidalgo, C., and De Freitas, M. S. (2007) Low expression of insulin signaling molecules impairs glucose uptake in adipocytes after early overnutrition. *J. Endocrinol.* **195**, 485–494
  38. Yen, C. L., Stone, S. J., Cases, S., Zhou, P., and Farese, R. V., Jr. (2002) Identification of a gene encoding MGAT1, a monoacylglycerol acyltransferase. *Proc. Natl. Acad. Sci. USA* **99**, 8512–8517
  39. Finck, B. N., and Hall, A. M. (2015) Does diacylglycerol accumulation in fatty liver disease cause hepatic insulin resistance? *BioMed Res. Int.* **2015**, 104132
  40. Saltiel, A. R., and Olefsky, J. M. (2017) Inflammatory mechanisms linking obesity and metabolic disease. *J. Clin. Invest.* **127**, 1–4
  41. Kayser, B. D., Goran, M. I., and Bouret, S. G. (2015) Perinatal overnutrition exacerbates adipose tissue inflammation caused by high-fat feeding in C57BL/6J mice. *PLoS One* **10**, e0121954
  42. Soufi, N., Hall, A. M., Chen, Z., Yoshino, J., Collier, S. L., Mathews, J. C., Brunt, E. M., Albert, C. J., Graham, M. J., Ford, D. A., and Finck, B. N. (2014) Inhibiting monoacylglycerol acyltransferase 1 ameliorates hepatic metabolic abnormalities but not inflammation and injury in mice. *J. Biol. Chem.* **289**, 30177–30188
  43. Hall, A. M., Soufi, N., Chambers, K. T., Chen, Z., Schweitzer, G. G., McCommis, K. S., Erion, D. M., Graham, M. J., Su, X., and Finck, B. N. (2014) Abrogating monoacylglycerol acyltransferase activity in liver improves glucose tolerance and hepatic insulin signaling in obese mice. *Diabetes* **63**, 2284–2296
  44. Agarwal, A. K., Tunison, K., Dalal, J. S., Yen, C. L., Farese, R. V., Jr., Horton, J. D., and Garg, A. (2016) *Mogat1* deletion does not ameliorate hepatic steatosis in lipodystrophic (*Agpat2<sup>-/-</sup>*) or obese (*ob/ob*) mice. *J. Lipid Res.* **57**, 616–630
  45. Raychaudhuri, N., Thamocharan, S., Srinivasan, M., Mahmood, S., Patel, M. S., and Devaskar, S. U. (2014) Postnatal exposure to a high-carbohydrate diet interferes epigenetically with thyroid hormone receptor induction of the adult male rat skeletal muscle glucose transporter isoform 4 expression. *J. Nutr. Biochem.* **25**, 1066–1076
  46. Park, J. H., Stoffers, D. A., Nicholls, R. D., and Simmons, R. A. (2008) Development of type 2 diabetes following intrauterine growth retardation in rats is associated with progressive epigenetic silencing of *Pdx1*. *J. Clin. Invest.* **118**, 2316–2324
  47. Sandovici, I., Smith, N. H., Nitert, M. D., Ackers-Johnson, M., Uribe-Lewis, S., Ito, Y., Jones, R. H., Marquez, V. E., Cairns, W., Tadayyon, M., O'Neill, L. P., Murrell, A., Ling, C., Constância, M., and Ozanne, S. E. (2011) Maternal diet and aging alter the epigenetic control of a promoter–enhancer interaction at the *Hnf4a* gene in rat pancreatic islets. *Proc. Natl. Acad. Sci. USA* **108**, 5449–5454
  48. Šeččíková, Z., Bujňáková, D., Raček, L., Kmet, V., and Možeš, Š. (2011) Developmental changes in gut microbiota and enzyme activity predict obesity risk in rats arising from reduced nests. *Physiol. Res.* **60**, 337–346
  49. Owen, C. G., Martin, R. M., Whincup, P. H., Davey-Smith, G., Gillman, M. W., and Cook, D. G. (2005) The effect of breastfeeding on mean body mass index throughout life: a quantitative review of published and unpublished observational evidence. *Am. J. Clin. Nutr.* **82**, 1298–1307
  50. Owen, C. G., Martin, R. M., Whincup, P. H., Smith, G. D., and Cook, D. G. (2006) Does breastfeeding influence risk of type 2 diabetes in later life? A quantitative analysis of published evidence. *Am. J. Clin. Nutr.* **84**, 1043–1054
  51. Yu, J. H., Lee, Y. J., Kim, H. J., Choi, H., Choi, Y., Seok, J. W., and Kim, J. W. (2015) Monoacylglycerol *O*-acyltransferase 1 is regulated by peroxisome proliferator-activated receptor  $\gamma$  in human hepatocytes and increases lipid accumulation. *Biochem. Biophys. Res. Commun.* **460**, 715–720

Received for publication July 27, 2017.  
Accepted for publication May 7, 2018.